**SUPPORTING INFORMATION**

# Real-Time Monitoring of Chromophore Isomerization and Deprotonation During the Photoactivation of the Fluorescent Protein Dronpa

Dheerendra Yadav,[a,b,c] Fabien Lacombat,[a,b,c] Nadia Dozova,[a,b,c] Fabrice Rappaport,[d] Pascal Plaza[a,b,c] and Agathe Espagne*[,a,b,c]

[a]Ecole Normale Supérieure-PSL Research University, Département de Chimie, 24 rue Lhomond, 75005 Paris, France

[b]Sorbonne Universités, UPMC Univ Paris 06, PASTEUR, F-75005, Paris, France

[c]CNRS, UMR 8640 PASTEUR, F-75005, Paris, France

[d]UMR 7141 CNRS-UPMC, Institut de Biologie Physico-Chimique, 13 rue Pierre et Marie Curie, 75005 Paris, France

Corresponding author: agathe.espagne@ens.fr

**Contents:**

## 1. Excited-state dynamics of OFF-state Dronpa-2 probed by broadband femtosecond UV-visible spectroscopy

The excited-state dynamics of OFF-state Dronpa-2 was probed by broadband femtosecond UV-visible spectroscopy, following 388-nm excitation with an energy of 40 nJ/pulse (6.6 µW, 166 Hz, ~$7\times10^4$ µm$^2$ spot size). Figure S1 displays the transient spectra for pump-probe delays ranging from 0.12 to 1200 ps. The spectra are similar to those of Dronpa and their temporal evolution involves the same three phases (see main text, §3.2). As in Dronpa, fast modifications of the shape of the excited-state spectrum are first observed (Figure S1, A and B), followed by a homothetic decay phase (Figure S1C). This latter is however a little slower than in Dronpa, extending up to 1.2 ns (Figure S1D).

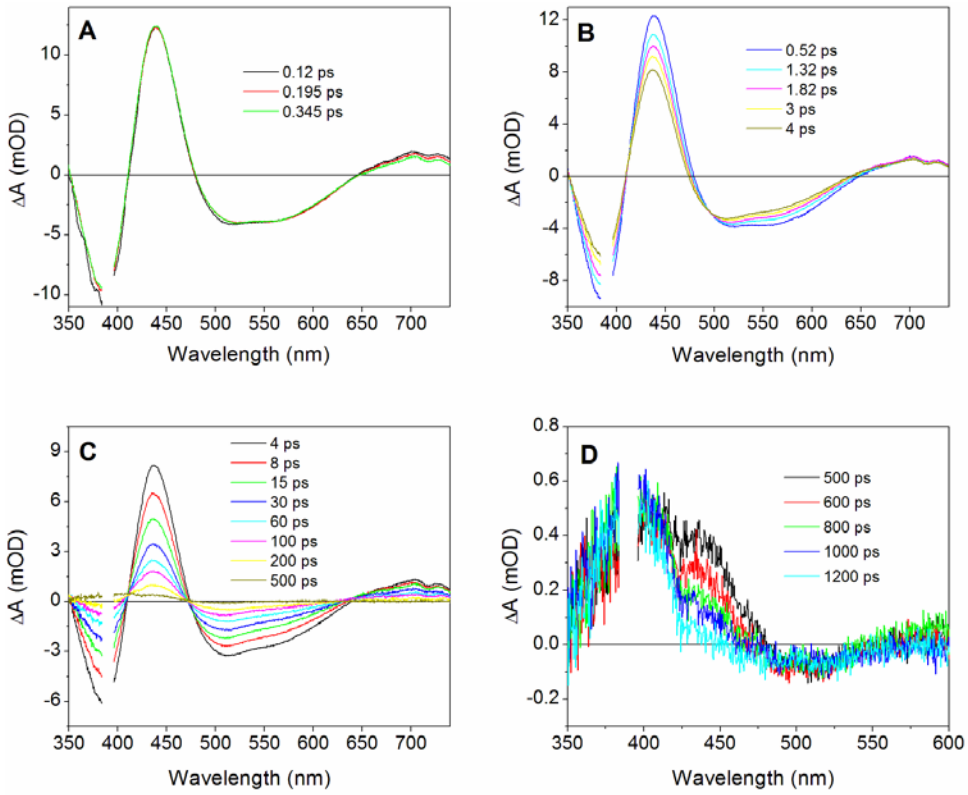


**Figure S1.** Transient absorption spectra of OFF-state Dronpa-2 in Tris buffer at pH 8.0 measured after excitation at 388 nm, for pump-probe delays ranging from A) 0.12 ps to 0.345 ps, B) 0.52 ps to 4 ps, C) 4 ps to 500 ps and D) 500 ps to 1200 ps. The data were corrected for the chirp of the probe.

The data were first globally fitted over the whole range of probed times, with best results obtained using two exponentials, a biexponential component and a plateau, like for Dronpa. The

lifetimes were found to be 0.22 ± 0.07 ps, 2.6 ± 0.2 ps, 15 ± 2 ps (60 %) and 160 ± 10 ps (40 %), the 15 ps and 160 ps lifetimes corresponding to the biexponential component. The DADS of the different components are shown in Figure S2A. In this fit, it appears that the spectrum of the plateau still contains a small contribution from the 440-nm excited-state absorption. It is thus not fully characteristic of the first ground-state photoproduct. This is in fact due to the existence of a fifth decay component that we could only fit properly by restricting the analysis to pump-probe delays longer than 500 ps. Its lifetime was then found to be 280 ± 140 ps. The associated DADS is shown in Figure S2B, together with the pure spectrum of the plateau.

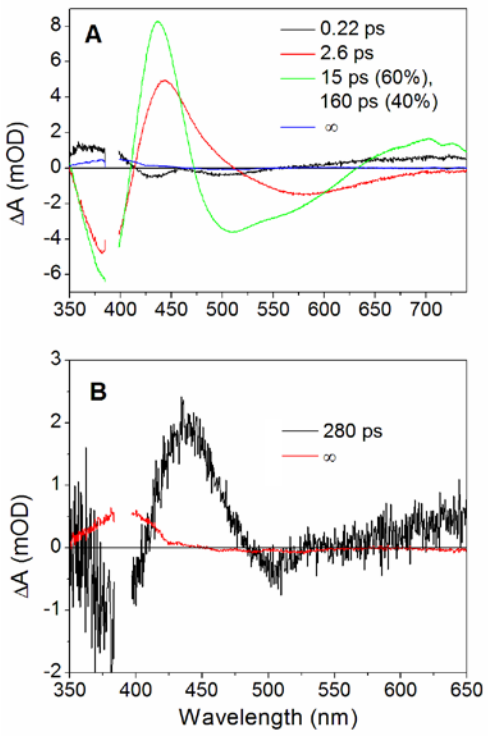


**Figure S2.** Amplitude spectra of the components (also called DADS, for decay-associated difference spectra) resulting from global kinetic analysis of OFF-state Dronpa-2 femtosecond data. A) Fit of the whole range of probed times with two exponentials, a biexponential component and a plateau. B) Fit of the 500 ps to 1.5 ns time range with one exponential and a plateau. These data were noise reduced by SVD (see main text, §2.3 of Methods).

## 2. Excitation energy dependence of the 600-ps transient absorption spectrum of OFF-state Dronpa

We found that the shape of the transient absorption spectrum of Dronpa at a few hundreds of picoseconds is particularly sensitive to the energy of the fs laser pulses used for excitation. This strong energy dependence is illustrated in Figure S3A. For pulses of less than 50 nJ (focused on a

section of ~$7\times10^4$ $\mu m^2$), the 600-ps transient absorption spectrum is identical to the DADS of the plateau commented in the main text. Two additional absorption contributions however appear at higher energies : a large band between 425 and 525 nm, with a peak at 455 nm, and a smaller and broader one beyond 525 nm.

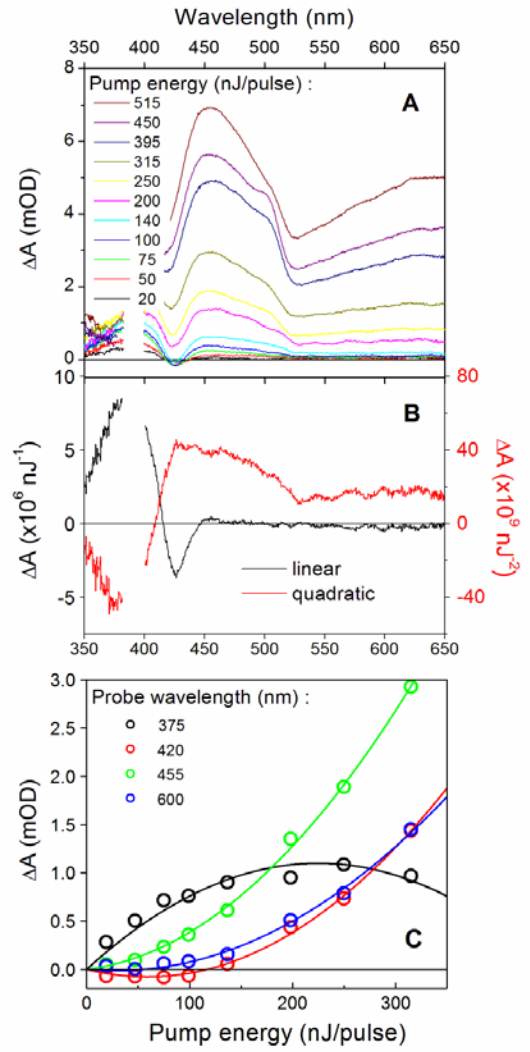


**Figure S3.** Pump energy dependence of the 600-ps transient absorption spectrum of Dronpa. A) 600-ps transient spectrum for pump energies ranging from 20 to 515 nJ/pulse. B) Spectra of the linear and quadratic contributions with respect to the pump energy, obtained by global fitting of the 600-ps data set with a second-order polynomial of the energy. These data were noise reduced by SVD (see main text, §2.3 of Methods). C) Pump energy dependence of the different bands in the 600-ps spectrum. The symbols correspond to the data and the lines to the second-order polynomial fit.

The broader band resembles the absorption spectrum of solvated electrons. Its slope in the 520 to 650 nm spectral range is however weaker than that reported in aqueous solution,[1,2] which

could be a feature of protein-solvated electrons. Such a flattened absorption has indeed also been observed for electrons putatively solvated inside the Photoactive Yellow Protein after multiphotonic photoionization of the chromophore.[3,4] If the absorption above 525 nm really corresponds to solvated electrons, it is expected that chromophore radicals formed at the same time also contribute to the signal. The formation of radicals and solvated electrons has been reported for the neutral GFP chromophore in solution, with radical absorption in the 400-500 nm spectral range.[5] The 455-nm absorption band could therefore be the signature of Dronpa chromophore radicals.

The question then arises as to how radicals and solvated electrons are formed in Dronpa. Figure S3C shows the energy dependence of the different bands contributing to the 600 ps transient signal. The 455-nm and 600-nm bands exhibit purely quadratic trends, while the 375-nm and 420-nm signals also show short linear regimes at low excitation energies ($\leq$ 50 nJ/pulse). These observations clearly show that a biphotonic mechanism is here at work, in parallel with the standard one-photon excitation. The data of Figure S3A were globally fitted with a second-order polynomial of the energy in order to extract the spectra associated with each contribution. These spectra are shown in Figure S3B. The linear spectrum is, as expected, virtually identical to the low-energy spectrum, while the quadratic spectrum consists of the above described absorptions of chromophore radicals and solvated electrons, plus the associated ground-state bleaching below 410 nm. We conclude that photoionization of OFF-state Dronpa is a two-photon process.

The quadratic spectrum of Figure S3B allows estimating the amount of two-photon products present in the samples at the 20 nJ/pulse pump energy we used for time-resolved photoactivation studies on Dronpa. At this energy, the absorption of chromophore radicals at 455 nm is expected to be ~$2\times10^{-6}$ OD. Such a signal lies far below the $5\times10^{-5}$ OD noise level of our time-resolved measurements, and is thus undetectable. According to femtosecond studies of the neutral GFP chromophore in solution,[5] the molar extinction coefficient of the radical is very close to the 21000 $mol^{-1}$ L $cm^{-1}$ extinction coefficient of hydrated electrons at 650 nm.[2] The concentration of chromophore radicals in our samples is therefore on the order of $9.5\times10^{-10}$ mol $L^{-1}$. Based on the excited concentration and photoactivation quantum yield measurements presented in the next sections (§3 and 4 of SI), we estimate the concentration of photoactivation intermediate X formed in the same conditions to be ~$1.8\times10^{-7}$ mol $L^{-1}$. We conclude that, after decay of the excited state,

the total transient population of our samples contains only ~0.5 % of two-photon products, which are not detected in the conditions of our time-resolved experiments.

### 3. Average concentration of excited molecules detected by the probe in femtosecond spectroscopy

In pump-probe spectroscopy, the pump creates a spatial concentration profile of excited molecules, due to its transverse energy profile at the sample. These excited molecules however do not all equally contribute to the pump-probe signal. Their contribution is proportional to the probe intensity they receive, which is determined by the probe transverse energy profile. In the linear regime, the pump-probe signal is therefore proportional to the concentration of excited molecules averaged over the product of the pump and probe beam profiles, a magnitude which we designate in short as the average concentration of excited molecules detected by the probe.

The average concentration of excited molecules detected by the probe was calculated based on the sample absorbance (A), the pump energy ($E_0$) and the normalized[†] pump and probe beam transverse profiles (P(x,y) and S(x,y), respectively) at the sample position. The beam profiles were recorded with 8.8 µm spatial resolution using a CCD camera (DataRay, WinCamD). This recording was done at the sample position, right after the pump-probe experiment and with the same alignment and spatial overlap of the beams. The calculations were performed numerically with Mathematica, using the raw beam profiles measured by the CCD. For simplicity all effects related to propagation of the beams in the sample are neglected. The sample is thus essentially considered as an infinitely thin surface on which all solute molecules are concentrated and where the pump and probe beams overlap.

Supposing excitation remains in the linear regime, the fraction $F_p$ of molecules excited by the pump at a particular position (x, y) of the sample plane is simply proportional to the pump density P and can be expressed as follows:

$$F_p(x,y) = \frac{N_0}{D} P(x,y).$$

In this expression, $N_0$ is the total number of pump photons absorbed by the sample and D is the surface density of molecules (in $cm^{-2}$). They are given by:

[†] The surface integral of the P(x,y) and S(x,y) profiles is equal to 1.

$$N_0 = \frac{E_0}{hc/\lambda}\left(1-10^{-A}\right)$$

and $$D = 10^{-3}\frac{A}{\varepsilon}N_{av},$$

with h the Planck constant, c the speed of light, λ = 388 nm the pump wavelength, ε the molar extinction coefficient of the sample at this wavelength (in $mol^{-1}$ L $cm^{-1}$) and $N_{av}$ Avogadro's number.

The average fraction of excited molecules detected by the probe, η, is then equal to the integral of $F_p$ weighted by the probe profile:

$$\eta = \iint F_p(x,y)S(x,y)dx\,dy = \frac{N_0}{D}\iint P(x,y)S(x,y)dx\,dy\,.$$

We found η to be of 0.01 to 0.02 in our experiments, that is much smaller than 1, which validates the linear pumping hypothesis. The average concentration of excited molecules detected by the probe, $C_{exc}$, is simply:

$$C_{exc} = \eta C_0\,,$$

with $C_0$ the total concentration of molecules in the sample. $C_{exc}$ determines the amplitude of the transient absorption signal.

To evaluate the accuracy of this approach for the estimation of excited concentrations, we applied it to the $[Ru(bpy)_3]^{2+}$ (tris-(2,2'-bipyridyl)ruthenium(II)) ruthenium complex, a photoactive system undergoing a well-characterized charge transfer reaction.[6,7] The metal-to-ligand charge transfer state of $[Ru(bpy)_3]^{2+}$ is formed in less than 1 ps and has a lifetime of several hundreds of nanoseconds.[6] The quantum yield of the reaction is one and the molar extinction coefficient of the charge transfer state is known,[7] which allows a second, independent determination of the average concentration of excited molecules detected by the probe. We found a discrepancy of 18 % between the values obtained by the two methods. We conclude that the error on the excited concentrations calculated by the beam profiles method, which was routinely used in this work, is of the order of ± 20 %.

The excited concentration values used to subtract the long-lived ground-state bleaching contributions of Dronpa (Figure 4) and Dronpa-2 (Figure S7) were 3.5 ± 0.7 µM and 5 ± 1 µM, respectively.

## 4. Experimental procedure for the determination of Dronpa and Dronpa-2 photoactivation quantum yields

We first measured the photoactivation rate constants of Dronpa and Dronpa-2 under continuous irradiation. For this purpose, 20-µL samples of OFF-state Dronpa or Dronpa-2 (20 µM in Tris-$H_2SO_4$ pH 8.0) were placed in a 1-mm optical path microcuvette (2-mm wide central channel, black sides). The samples were irradiated for defined time intervals with continuous light from a xenon lamp (Linos LQX1800) reflected by a dichroïc mirror (reflection < 450 nm) and passed through an interference filter (Semrock 360/12), resulting in UV light centered at 364 nm and of 10-nm FWHM spectral width. The irradiation times (20 to 600 ms for actinometry (see below) and up to 20 s for photoactivation) were controlled by a mechanical shutter integrated in the lamp and computer-controlled via a data acquisition board (National Instruments). The absorption spectra of the samples were recorded after each illumination to monitor the OFF→ON conversion, and these illumination/recording cycles were repeated 5 to 10 times (Figure S4 A and B).

For Dronpa, the photoactivation rate constant $k_{Dronpa}$ was simply taken as the opposite of the slope of $\ln(A_{388}) = f(t)$ (Figure S4A, inset). In the case of Dronpa-2, the effective rate constant of OFF→ON conversion ($k_{eff}$) results both from the photoactivation process ($k_{Dronpa\text{-}2}$) and from spontaneous return of the OFF state to the ON state ($k_{th}$).[8,9] It can easily be shown that $k_{eff} = k_{Dronpa\text{-}2} + k_{th}$. We followed the spontaneous conversion in the dark by spectrophotometry (Figure S4C) and found $k_{th} = 2.74\times10^{-3}$ $s^{-1}$, corresponding to a characteristic time of 6.1 min (at 20°C). The photoactivation rate constant $k_{Dronpa\text{-}2}$ was taken as $k_{eff} - k_{th}$.

The excitation rate constant ($k_{exc}$) was then measured by monitoring the photolysis of the chemical actinometer DMAD[10] (p-(dimethylamino)benzenediazonium; 25 µM in 50 mM $H_2SO_4$) under exactly the same irradiation conditions (same cuvette and illumination setup), following a standard method of photon flux determination.[11,12] The absorption spectra of DMAD recorded after successive irradiations are shown in Figure S4D, together with its 378-nm photolysis kinetics (inset). $k_{exc}$ was deduced from the photolysis rate constant of DMAD ($k_{DMAD}$) using $k_{exc} = k_{DMAD}/\Phi_{DMAD} \times \varepsilon_{Dronpa}/\varepsilon_{DMAD}$, as previously described.[12,13] We took $\Phi_{DMAD} = 0.57$,[10] $\varepsilon_{DMAD} = 27120$ $mol^{-1}$ L $cm^{-1}$ (average over our spectral range of irradiation, with the published extinction coefficient of 36100 $mol^{-1}$ L $cm^{-1}$ at 378 nm[10]) and the OFF-state molar extinction coefficients of Dronpa and Dronpa-2 shown in Table 1 (main text). In the conditions of this study, $k_{exc}$ was

typically of 0.48 $s^{-1}$ for Dronpa and 0.31 $s^{-1}$ for Dronpa-2. It was cross-checked using a second chemical actinometer, α-(p-dimethylaminophenyl)-N-phenylnitrone,[14] and a power-meter. The photoactivation quantum yields $\Phi_{Dronpa}$ and $\Phi_{Dronpa\text{-}2}$ were finally obtained as the ratio of $k_{Dronpa}$, respectively $k_{Dronpa\text{-}2}$, to $k_{exc}$.

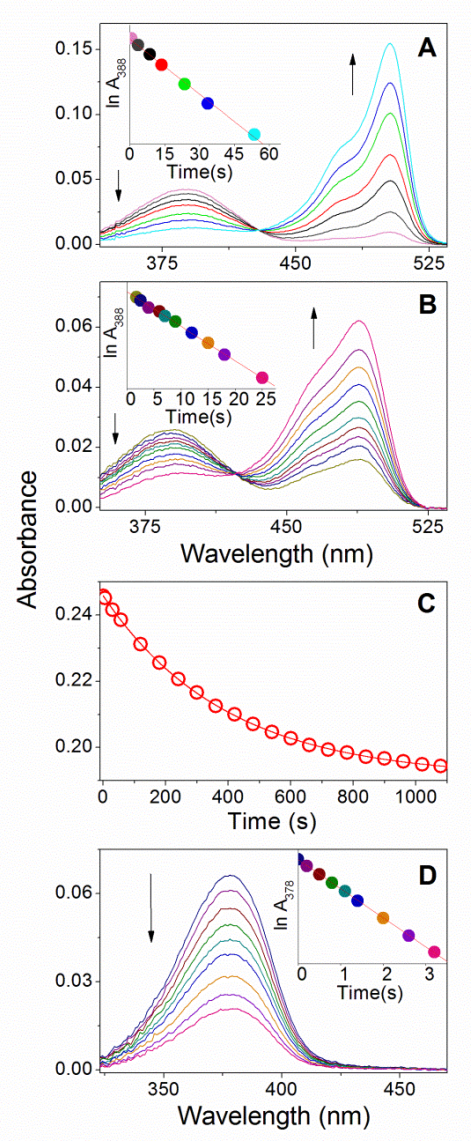


**Figure S4.** Determination of the photoactivation quantum yields of Dronpa and Dronpa-2. A) and B) Photoactivation of Dronpa and Dronpa-2. Absorption spectra recorded after successive periods of continuous irradiation with 364-nm light. Inset: logarithm of 388-nm absorption as a function of total irradiation time (symbols, using the same colors as the corresponding spectra) and linear regression line. C) Spontaneous OFF→ON conversion of Dronpa-2 in the dark. 388-nm absorption as a function of time (symbols) and exponential fit (line). D) DMAD actinometry. Absorption spectra recorded after successive periods of irradiation in the same conditions as Dronpa and Dronpa-2. Inset: logarithm of 378-nm absorption as a function of total irradiation time (symbols, using the same colors as the corresponding spectra) and linear regression line.

## References


(1) Jou, F. Y.; Freeman, G. R. Temperature and Isotope Effects on the Shape of the Optical-Absorption Spectrum of Solvated Electrons in Water. *J. Phys. Chem.* **1979**, *83*, 2383-2387.

(2) Hare, P. M.; Price, E. A.; Bartels, D. M. Hydrated electron extinction coefficient revisited. *J. Phys. Chem. A* **2008**, *112*, 6800-2.

(3) Larsen, D. S.; van Stokkum, I. H. M.; Vengris, M.; van der Horst, M. A.; de Weerd, F. L.; Hellingwerf, K. J.; van Grondelle, R. Incoherent manipulation of the photoactive yellow protein photocycle with dispersed pump-dump-probe spectroscopy. *Biophys. J.* **2004**, *87*, 1858-1872.

(4) Changenet-Barret, P.; Plaza, P.; Martin, M. M.; Chosrowjan, H.; Taniguchi, S.; Mataga, N.; Imamoto, Y.; Kataoka, M. Structural effects on the ultrafast photoisomerization of Photoactive Yellow Protein. Transient absorption spectroscopy of two point mutants. *J. Phys. Chem. C* **2009**, *113*, 11605-11613.

(5) Vengris, M.; van Stokkum, I. H. M.; He, X.; Bell, A. F.; Tonge, P. J.; van Grondelle, R.; Larsen, D. S. Ultrafast Excited and Ground-State Dynamics of the Green Fluorescent Protein Chromophore in Solution. *J. Phys. Chem. A* **2004**, *108*, 4587-4598.

(6) Damrauer, N. H.; Cerullo, G.; Yeh, A.; Boussie, T. R.; Shank, C. V.; McCusker, J. K. Femtosecond dynamics of excited-state evolution in [Ru(bpy)(3)](2+). *Science* **1997**, *275*, 54-57.

(7) Yoshimura, A.; Hoffman, M. Z.; Sun, H. An Evaluation of the Excited-State Absorption-Spectrum of Ru(Bpy)3(2+) in Aqueous and Acetonitrile Solutions. *J. Photochem. Photobiol. A* **1993**, *70*, 29-33.

(8) Stiel, A. C.; Trowitzsch, S.; Weber, G.; Andresen, M.; Eggeling, C.; Hell, S. W.; Jakobs, S.; Wahl, M. C. 1.8 A Bright-State Structure of the Reversibly Switchable Fluorescent Protein Dronpa Guides the Generation of Fast Switching Variants. *Biochem. J.* **2007**, *402*, 35-42.

(9) Ando, R.; Flors, C.; Mizuno, H.; Hofkens, J.; Miyawaki, A. Highlighted Generation of Fluorescence Signals Using Simultaneous Two-Color Irradiation on Dronpa Mutants. *Biophys. J.* **2007**, *92*, L97-L99.

(10) Cox, R. J.; Bushnell, P.; Evleth, E. M. Photophysical and Photochemical Properties of Sterically Hindered Aryldiazonium Salts. *Tetrahedron Lett.* **1970**, 207-210.

(11) Kuhn, H. J.; Braslavsky, S. E.; Schmidt, R. Chemical Actinometry. *Pure Appl. Chem.* **2004**, *76*, 2105-2146.

(12) Thiagarajan, V.; Villette, S.; Espagne, A.; Eker, A. P. M.; Brettel, K.; Byrdin, M. DNA repair by photolyase: a novel substrate with low background absorption around 265 nm for transient absorption studies in the UV. *Biochemistry* **2010**, *49*, 297-303.

(13) Yamamoto, J.; Martin, R.; Iwai, S.; Plaza, P.; Brettel, K. Repair of the (6-4) Photoproduct by DNA Photolyase Requires Two Photons. *Angew. Chem. Int. Ed.* **2013**, *52*, 7432-7436.

(14) Wang, P. F.; Jullien, L.; Valeur, B.; Filhol, J.-S.; Canceill, J.; Lehn, J.-M. Multichromophoric cyclodextrins. 5. Antenna-induced unimolecular photoreactions. Photoisomerization of a nitrone. *New J. Chem.* **1996**, *20*, 895-907.

## 5. Additional supplementary figures (S5 to S8)

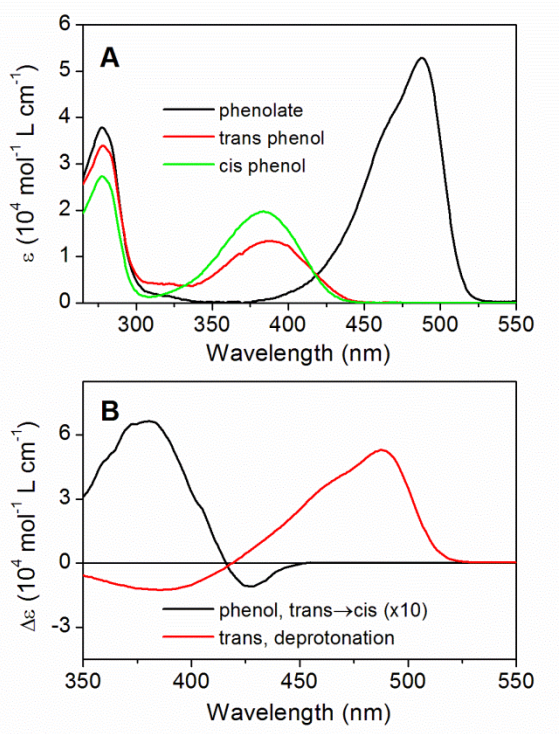


**Figure S5.** A) Absorption spectra of the different forms of the Dronpa-2 chromophore: cis- and trans-phenolate (indistinguishable), trans-phenol and cis-phenol. B) Difference spectra associated with trans→cis isomerization of a phenol chromophore (cis-phenol minus trans-phenol; 10× magnified) and with deprotonation of a trans chromophore (trans-phenolate minus trans-phenol). The data were smoothed over 11 points using Savitzky-Golay algorithm with a second order polynomial.

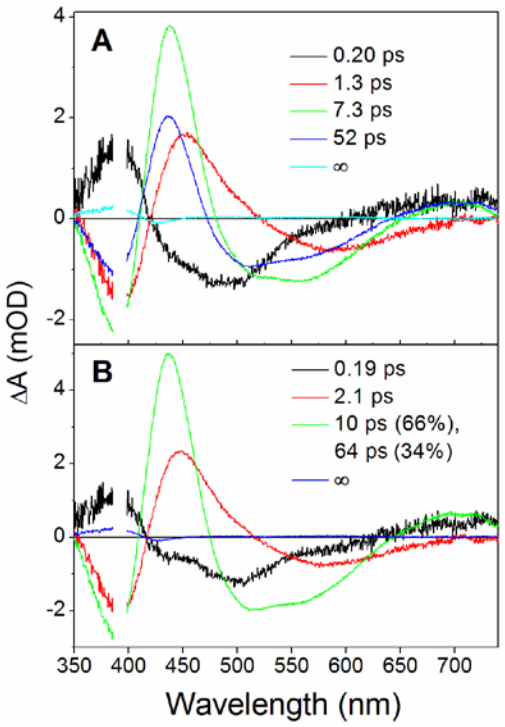


**Figure S6.** Amplitude spectra of the components (also called DADS, for decay-associated difference spectra) resulting from global kinetic analysis of OFF-state Dronpa femtosecond data using two models: A) four exponentials plus a plateau; B) two exponentials, a biexponential component plus a plateau. These data were noise reduced by SVD (see main text, §2.3 of Methods).

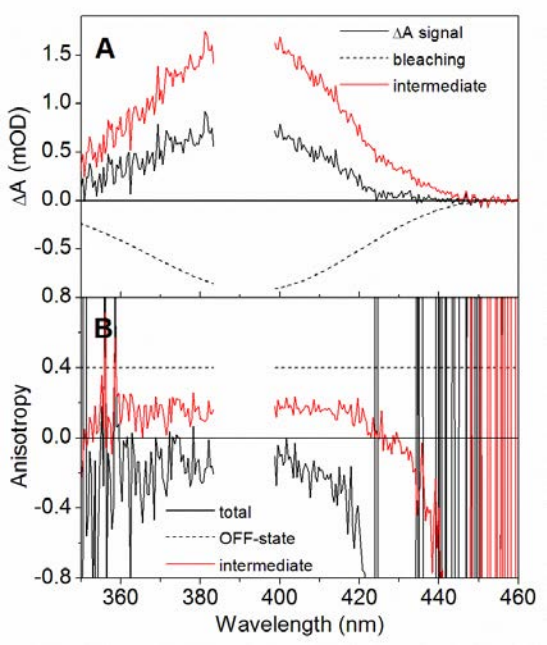


**Figure S7.** A) Decomposition of the long-lived isotropic spectrum of Dronpa-2 (DADS of the plateau) into ground-state bleaching and intermediate absorption. B) Total long-lived anisotropy, OFF-state anisotropy and anisotropy of the intermediate deduced from the spectral decomposition of the isotropic data. These data were noise reduced by SVD (see main text, §2.3 of Methods).

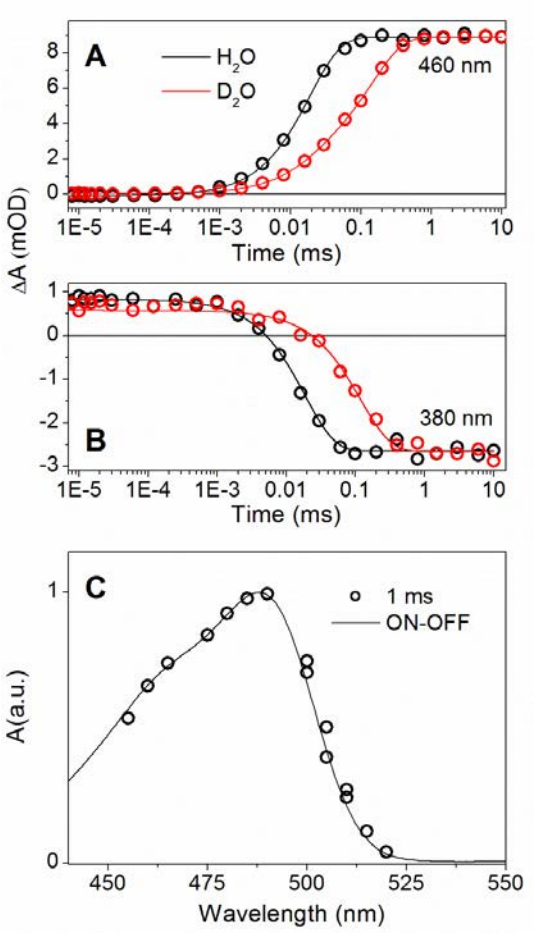


**Figure S8.** Nano- to millisecond transient absorption spectroscopy of OFF-state Dronpa-2. The samples were excited at 425 nm. A) Kinetics measured at 460 nm in aqueous and deuterated Tris buffers of pH/pD 8.0. The symbols correspond to the raw data and the lines to multiexponential fits with average lifetimes of 19 µs for the $H_2O$ sample and 124 µs for the $D_2O$ sample. We tentatively attribute the multiexponential character of the deprotonation kinetics of Dronpa-2 to the larger conformational freedom of the chromophore than in Dronpa. B) Kinetics measured at 380 nm in the same buffers. C) 1-ms transient absorption spectrum in the 460 to 520 nm spectral range overlapped with the ON minus OFF difference spectrum (cis-phenolate minus trans-phenol).